Seismic modeling of acid-gas injection in a deep saline reservoir

Charles P. Ursenbach and Donald C. Lawton

ABSTRACT

A number of projects involve the injection of acid gas into non-commercial reservoirs as a means of disposal. Acid gas removed from natural gas is composed of carbon dioxide, hydrogen sulfide, methane, and other residual gaseous hydrocarbons. It may also contain water, but this is often removed prior to acid-gas injection.

A case is studied of non-aqueous acid gas injection into a saline dolostone reservoir. Seismic monitoring of an injection plume requires knowledge of acid gas acoustic properties, and for a non-aqueous acid gas these can be calculated using the Peng-Robinson equation of state. Gassmann's equation can then be used to describe fluid substitution, if the assumptions of Gassmann's equation are valid. However the assumption that fluids do not interact with the rock matrix must be considered carefully in view of the acidity of the injected fluid, particularly for carbonate rocks. Studies have not yet clarified the rate of reaction of acid gas with carbonate rocks. However, a mineral such as dolomite will react more slowly than calcite, and it is therefore reasonable to assume that substantial reaction will occur on a longer time scale than the early stages of injection. This would justify using the standard Gassmann's equation to monitor initial injection progress.

The feasibility of monitoring is judged by the sensitivity of traveltimes and reflection coefficients to fluid substitution. Using acid-gas properties from the Peng-Robinson equation of state and fluid substitution effects from Gassmann's equations, the traveltime difference is seen to be on the order of a quarter millisecond for each 10 m thickness of the acid-gas plume for average dolostone properties, and up to a half millisecond for softer dolostones. Minor changes in reflection coefficient are also observed, but full analysis with well logs would be required for a useful assessment of this effect.

INTRODUCTION

Carbon dioxide (CO_2) and hydrogen sulfide (H_2S) are common byproducts of the energy industry. A course of remediation which is being explored is to sequester them in subsurface reservoirs. Deep saline reservoirs are one attractive target. Acid gas injection is becoming a method of choice (as a replacement for flaring) at smaller gas wells where it is not economical to build traditional facilities for scrubbing. For such injection programs to work it would be desirable to track the progress of the injection plume via seismic monitoring. To study the feasibility of monitoring, one should first carry out modeling studies of fluid substitution, to gain insight into the ability of the seismic method to distinguish pre- and post-injection states of the reservoir medium. The purpose of this study is to carry out fluid substitution calculations for the modeling of an injection process.

Seismic fluid substitution modeling is commonly based on the Gassmann equation, which requires knowledge of density and moduli for the rock matrix and for its fluid contents, both before and after injection. It also rests upon certain assumptions, and in a non-standard application such as this it may be important to revisit the validity of some assumptions. In particular it is important to consider whether there is interaction between fluid and rock matrix, which is assumed to be absent in the Gassmann formulation. At least two types of interaction with acidified fluids are conceivable: dissolution of carbonate minerals, and precipitation of carbonates in the presence of basic aluminosilicate minerals (Holloway, 2007). The case we will consider involves the carbonate mineral dolomite, which could then undergo dissolution. This would occur at a slower rate than, say, calcite, and we assume in this initial study that this process will occur on a longer time scale than the injection program, in which case the non-interaction assumption would be valid for the present study. This question would of course be more significant in monitoring long-term storage than in monitoring the initial injection.

In studying fluid substitution it is also important to know in what manner the native and injected fluids interact. Three possible modes are displacement (in which the flooded region contains 100% injected gas), heterogeneous mixing (which results in a patchy mixture of native and injected gases), and dissolution (in which the two fluids are mixed to form a new homogeneous fluid). Holloway (2007) suggests that the time of dissolution could be on the order of a few thousand years, so we will not consider this mode. For simplicity we will assume a model in which brine is initially wholly displaced by acid gas in the injection process, and will defer consideration of patchy mixing to a future study.

PROBLEM STATEMENT

Given information on a deep saline reservoir, and on an injected acid gas, we wish to carry out fluid substitution calculations in order to assess whether surface seismic may be feasibly used to monitor progress of the injection plume.

The following information is given: For the reservoir we know temperature, pressure, porosity, and general lithology. We also know the salinity of the pre-existing brine. We do not know exact thickness and do not possess well logs. For the acid gas we know composition (including that it is non-aqueous). A typical set of known information is given in Table 1.

Table 1. Known parameters relating to fluid injection problem.

Reservoir Parameters		Acid Gas Parameters	
Temperature	40°C	Composition (mole fraction):	
Pressure	9465 kPa	Carbon dioxide (CO_2)	0.745
Porosity	0.10	Hydrogen sulfide (H_2S)	0.193
Lithology	Dolostone	Water (H_2O)	0
Salinity	120,000 ppm		
Thickness estimate	8 – 30 m		

The above information represents one case of interest that will be used for concreteness; however this report is more concerned with developing methodology that may be applied or adapted to a variety of acid-gas injection scenarios.

PROPOSED METHOD

Given the information above, the general approach to this problem will consist of the following steps:

1) Determine acoustic properties (at reservoir temperature and pressure) of relevant fluids. Normally for the present case this would consist of only the pre-existing brine and the injected acid gas, but as we will see, in this instance, the properties of non-saline water will be required as well.

2) Obtain elastic properties of the reservoir rock for some reference saturated state, and the elastic properties of the mineral(s) comprising it. Normally the reference state would be the original brine-saturated state, but because of the absence of well logs, we will choose the water-saturated state as a reference, as we can estimate its elastic properties from existing literature.

3) Determine the change in reservoir elastic properties due to fluid substitution via Gassmann's equation.

We will consider each of these steps in detail

Determining fluid properties

Three fluids are of interest in this case, water, brine and non-aqueous acid gas.

Properties of water and brine

The acoustic properties of water and brine (i.e. density and P-wave velocity) are readily determined from available empirical relations, if the salinity of the brine is known and is due to the species NaCl. These expressions are available, for instance, in Batzle and Wang (1992) or Mavko et al. (1998).

Properties of acid gas

Acid-gas, while a key player in refining operations, has not been much on the exploration or development radar before now. Thus its acoustic properties have not been well-investigated. We will therefore describe in detail the method employed for calculation of these properties.

A variety of approaches are possible for calculating properties of acid gas. We follow the recommendation of Carroll (2002a) who has shown that the Peng-Robinson equation of state (Peng and Robinson, 1976) provides an adequate description of non-aqueous acid gas. If water is present, then further modifications are required (Carroll, 1992, 2002b). The presence of water in acid gas adds the additional complication that CO_2, H_2S and CH_4 all form solid hydrates (Carroll, 1998). The system we consider here involves only a non-aqueous acid gas.

An equation of state is typically expressed as $P = P(T,v,\{x_i\})$, where P is pressure, T is temperature, v is molar volume, and x_i is the mole fraction of the i^{th} species. In detail the Peng-Robinson equation of state is written

$$P = \frac{RT}{v-b} - \frac{a(T)}{v(v+b)+b(v-b)} \tag{1}$$

where the constant b and the temperature-dependent function $a(T)$ are defined in Appendix A.

Given T, v and $\{x_i\}$ it is straightforward to calculate P from equation 1. In this application however we begin with T, P and $\{x_i\}$ and seek to calculate the density (ρ) and the bulk modulus (K). From these we can also calculate the speed of sound (V_P). The procedure for doing this is described by Batzle and Wang (1992) and is outlined in Figure 1. We describe below each of the steps in Figure 1 in more detail.

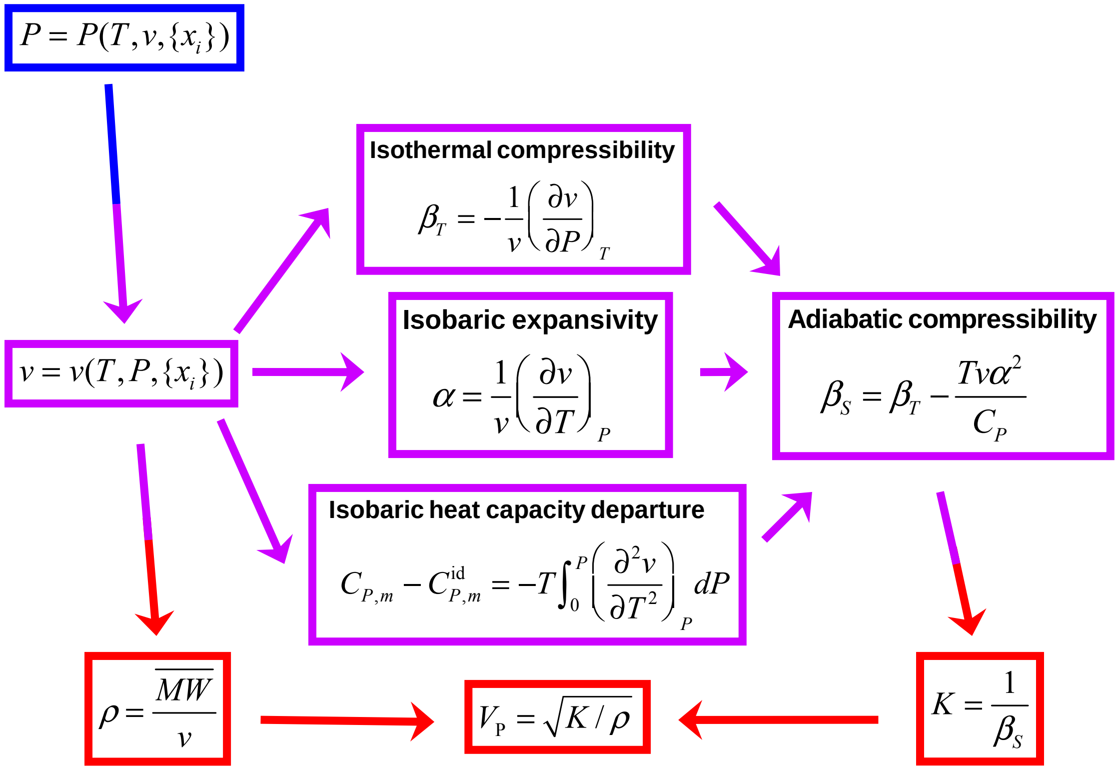

FIG. 1. A flow diagram outlining the procedure for obtaining fluid acoustic properties from a *P-V-T* equation of state. The composition, $\{x_i\}$, is assumed to be held constant in all differentiations and integrations.

1) Molar volume – Equation 1 can be solved for v by rearranging it into a cubic equation and applying standard solution methods (e.g. Press et al., 1988).

$$Pv^3 + (Pb - RT)v^2 + [a(T) - 3Pb^2 - 2RTb]v + b[Pb^2 + RTb - a(T)] = 0 \qquad (2)$$

A cubic equation possesses either one or three real solutions. If there is one solution, then the acid gas is either gas, liquid, or a supercritical fluid. If there are three solutions then the acid gas is on or near a gas-liquid phase coexistence line. In this latter case the larger real solution is the gaseous molar volume and the smaller is the liquid molar volume.

2) Density – The average molar weight, $\overline{MW} = \sum_i x_i (MW)_i$, divided by the molar volume, v, yields the mass density, ρ.

3) Isothermal compressibility – Differentiating equation 2 with respect to P at constant T and then solving for $(\partial v/\partial P)_T$ allows one to construct an analytic expression for the isothermal compressibility.

4) Isobaric thermal expansivity – As in the preceding item, one can differentiate equation 2 with respect to T at constant P and then solve for $(\partial v/\partial T)_P$. This is the

central component of the isobaric expansivity. This procedure is slightly more complicated than obtaining the compressibility, however, as the differentiation will also involve derivatives of $a(T)$. The precise form of $a(T)$ is given in Appendix A.

5) Heat capacity departure – The difference between real and ideal isobaric heat capacities can be expressed as an integral, as indicated in Figure 1 (Sandler, 1999, eq. 4.4-10). In practice it is more convenient to convert it into an integral over v, as shown in Appendix B. In the next step the full heat capacity, including the ideal contribution, is required. This may be calculated from data on molecular geometries and vibrational frequencies, as described in Appendix C.

6) Adiabatic compressibility – Sound waves pass too quickly through earth media to allow for significant dissipation of energy. Therefore they are associated with adiabatic rather than isothermal compressions and dilations. The adiabatic compressibility can be computed using the standard thermodynamic relation in Figure 1.

7) Bulk modulus – The reciprocal of the adiabatic compressibility yields the bulk modulus.

The above computations were implemented as a Java applet for distribution to sponsors, for acid gases composed of an arbitrary mixture of CO_2, H_2S, N_2, methane, ethane, and propane. This applet also implements calculations of other pore fluids, as described in Batzle and Wang (1992).

Determining reservoir rock properties

Normally the elastic properties of a reservoir are estimated from well-log data, especially if P-wave and S-wave sonic logs are available. This section addresses the case when such data is not available. In this case we can make use of literature data to estimate reasonable values for the elastic properties of water-saturated dolomite of known porosity.

Our source for literature data is Mavko et al. (1998), p. 292-293. Graphs are presented there for correlation of various quantities, along with best-fit correlations. The three results of interest to us are

$$V_\mathrm{P}\,[\mathrm{km/s}] = 6.6067 - 9.3808\phi \tag{3}$$

$$V_\mathrm{S}\,[\mathrm{km/s}] = 3.5817 - 4.7194\phi \tag{4}$$

$$\rho\,[\mathrm{g/cm^3}] = 1.8439 + 0.13786 V_\mathrm{P} \tag{5}$$

Thus for a given porosity one can estimate three typical elastic properties for water-saturated dolomite. From the scatter of data in the graphs, one can also visually estimate an uncertainty in each of these values.

The data employed in forming equations 3-5 was obtained at a variety of pressures (10, 15 and 35 MPa). As a future refinement, one could contemplate using the pressure of the reservoir to more narrowly and correctly define these estimates.

We also require elastic properties (or at least bulk modulus and density) of the mineral dolomite, $CaMg(CO_3)_2$, of which the rock matrix is composed. Again we turn to data from Mavko et al. (1998, p. 308) which lists three values for these properties. We have used the average of all listed values for our calculation.

Fluid substitution calculations

The most common (though not the only) approach to performing fluid substitution calculations is to use the Gassmann equation (Mavko et al., 1998):

$$K_{\mathrm{satd}} = K_{\mathrm{skel}} + \frac{\left(1 - \dfrac{K_{\mathrm{skel}}}{K_{\mathrm{mineral}}}\right)^2}{\dfrac{\phi}{K_{\mathrm{fluid}}} + \dfrac{1-\phi}{K_{\mathrm{mineral}}} - \dfrac{K_{\mathrm{skel}}}{K_{\mathrm{mineral}}^2}} . \qquad (6)$$

This expresses, subject to various assumptions, the bulk modulus of a fluid-saturated rock (K_{satd}) with porosity ϕ in terms of the bulk moduli of the dry rock skeleton (K_{skel}), the mineral of which the skeleton is composed (K_{mineral}), and the saturating fluid (K_{fluid}).

It is useful in fluid substitution exercises to be able to solve for the bulk modulus of the dry rock skeleton, K_{skel}. This inversion can be carried out analytically in the following way. First, rewrite equation 6 without K_{skel} by defining a new quantity α:

$$K_{\mathrm{satd}} = K_{\mathrm{mineral}}(1-\alpha) + \frac{\alpha^2}{\dfrac{\phi}{K_{\mathrm{fluid}}} + \dfrac{\alpha-\phi}{K_{\mathrm{mineral}}}}, \qquad \alpha \equiv 1 - \frac{K_{\mathrm{skel}}}{K_{\mathrm{mineral}}} .$$

Next, rearrange this result to isolate α. The result is

$$\alpha = \frac{\dfrac{K_{\mathrm{mineral}}}{K_{\mathrm{fluid}}} - \dfrac{K_{\mathrm{satd}}}{K_{\mathrm{fluid}}} + \dfrac{K_{\mathrm{satd}}}{K_{\mathrm{mineral}}} - 1}{\dfrac{K_{\mathrm{mineral}}}{K_{\mathrm{fluid}}}\phi + \dfrac{K_{\mathrm{satd}}}{K_{\mathrm{mineral}}} - \phi - 1}\phi .$$

Finally, replace α with its definition and rearrange to isolate K_{skel}:

$$K_{\mathrm{skel}} = \frac{K_{\mathrm{satd}}\left(1 - \phi + \dfrac{K_{\mathrm{mineral}}}{K_{\mathrm{fluid}}}\phi\right) - K_{\mathrm{mineral}}}{\dfrac{K_{\mathrm{mineral}}}{K_{\mathrm{fluid}}}\phi + \dfrac{K_{\mathrm{satd}}}{K_{\mathrm{mineral}}} - \phi - 1} . \qquad (7)$$

This result is attributed to Zhu and McMechan (1990).

Before using equations 6 and 7 for fluid substitution, first note that K_{mineral}, K_{skel}, and ϕ do *not* change with different fluids in the pore. (One could argue this, but, as discussed in the introduction, it will be assumed for the present study.) On the other hand, K_{fluid} and K_{satd} *do* change with a change in fluid.

To carry out fluid substitution, we begin with the reference state. The known properties of water-saturated dolomite (K_{fluid}(water), K_{satd}(water), K_{mineral}, and ϕ) are substituted into equation 7 to obtain K_{skel}. Then we use equation 6 with known values of K_{fluid}(brine) and K_{fluid}(acid gas) to obtain K_{satd}(brine) and K_{satd}(acid gas).

One also needs to find how shear-wave properties and density change with fluid substitution. This is somewhat less involved than finding K_{satd}. The shear modulus is (under Gassmann assumptions) invariant to the fluid, so that $\mu_{\text{skel}} = \mu_{\text{satd}}$(water) $= \mu_{\text{satd}}$(brine) $= \mu_{\text{satd}}$(acid gas), where $\mu = \rho V_S^2$. The fluid dependence of density is given by the equation

$$\rho_{\text{satd}} = \rho_{\text{skel}} + \phi\, \rho_{\text{fluid}}. \tag{8}$$

This can be used with data for the water-saturated state to obtain ρ_{skel}, and then with brine and acid gas fluid data to obtain ρ_{satd}(brine) and ρ_{satd}(acid gas). Alternatively, ρ_{skel} can be first obtained from

$$\rho_{\text{skel}} = (1-\phi)\rho_{\text{mineral}} \tag{9}$$

Once one has all elastic properties for the brine and acid-gas saturated states, one can obtain velocities as well, and then one can perform seismic modeling to assess whether seismic monitoring will be able to follow progress of the injection plume.

RESULTS

We have used the data of Table 1 and the prescriptions of the previous section to calculate elastic properties after fluid substitution. As the composition of the acid gas is not fully defined in Table 1, it is assumed that the remaining 6.2% consists of methane gas. The results are collected in Table 2.

Table 2. The following results are obtained using the parameters of Table 1. Digits in brackets in the final two rows should be rounded, and are given only to show the progress of the calculations.

Medium	ρ (g/cm^3)	K (GPa)	μ (GPa)	V_P (km/s)	V_S (km/s)
Fluid properties					
Water	0.9957	2.377	-	1.545	-
Brine	1.081	3.008	-	1.668	-
Acid gas	0.432	0.0332	-	0.277	-
Reservoir rock properties					
Dolomite mineral	2.87	80.1	48.7	7.11	4.12
Water sat'd dolostone (typical value)	2.6	51	25	5.7	3.1
Water sat'd dolostone (normal range)	2.5-2.7	-	-	5.2-6.2	2.7-3.7
Fluid substitution results					
Brine sat'd dolostone	2.6(1)* 2.6(9)**	53.(8)	25	5.7(8)* 5.6(9)**	3.0(9)* 3.0(5)**
Acid gas sat'd dolostone	2.5(4)* 2.6(3)**	40.(0)	25	5.3(7)* 5.2(8)**	3.1(3)* 3.0(8)**

* Result using equation 8 ** Result using equation 9

APPLICATION OF RESULTS

Monitoring fluid substitution in the subsurface can be accomplished by a variety of methods, depending on what properties are most sensitive to a change in fluid. Two characteristics of seismic data that can be influenced are traveltime through the reservoir and amplitude variation with offset (AVO) at the top or bottom of the reservoir.

Traveltime calculations

The difference in two-way traveltime for a P-wave traveling vertically through a reservoir containing either brine or acid gas is given by

$$\Delta T = 2d\left(\frac{1}{V_P(\text{acid gas})} - \frac{1}{V_P(\text{brine})}\right), \tag{10}$$

where d is the thickness of the reservoir. Using data from Table 2 we find that there is a 0.26 ms increase in two-way traveltime after fluid substitution, for each 10 m thickness of the reservoir. This result is unaffected by whether equation 8 or 9 is used in the calculation.

Because precise information is not available on the elastic properties of the reservoir, it is also of interest to see how this traveltime difference estimate varies with properties of the reservoir. To accomplish this, the calculations of Table 2 and equation 10 were re-executed several times for various values of V_P from 5.2 to 6.2 km/s. The results are shown in Figure 2.

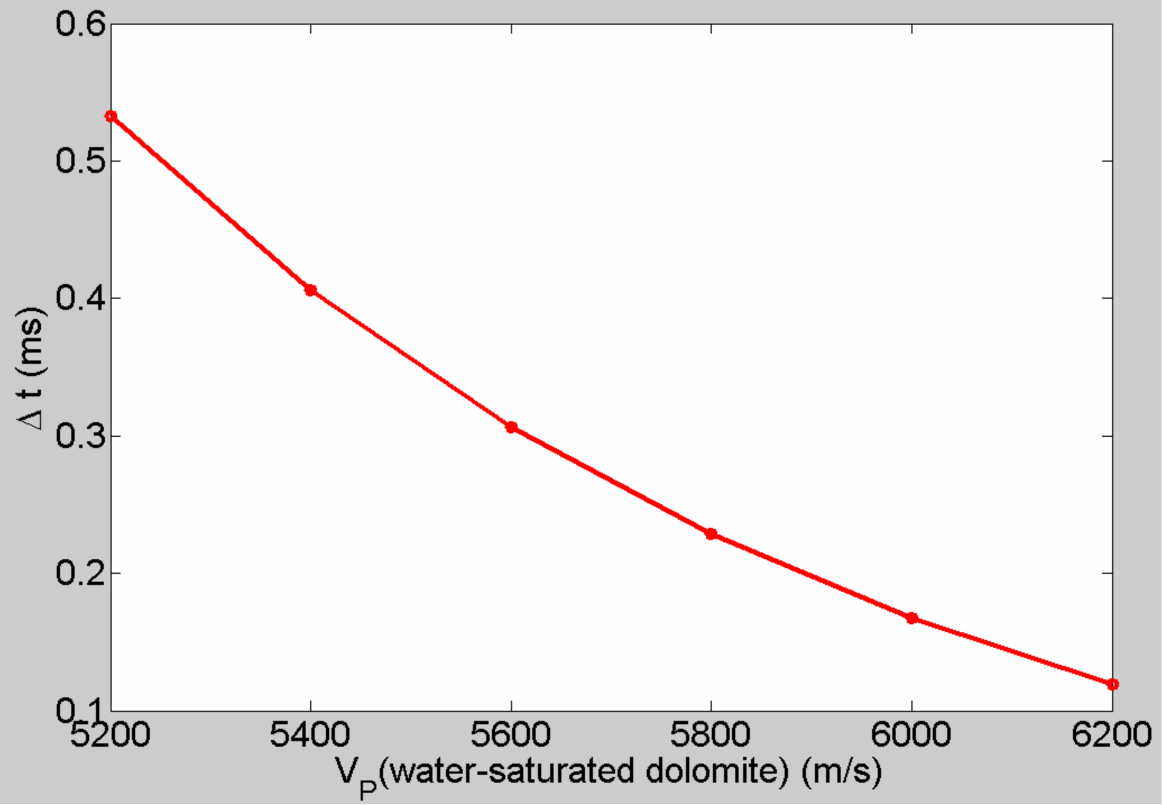

FIG. 2. The effect of reservoir rock V_P on two-way traveltime differences resulting from fluid substitution.

For the softer end of the range, traveltime differences are about 0.5 ms per 10 m thickness of the reservoir. This is a measureable amount and suggests that seismic monitoring may be feasible. Of course if V_P is at the lower end of its range, then V_S and ρ, which are positively correlated with V_P, are likely at the lower end of their ranges as well. However, if we recalculate Figure 2, adjusting V_S and ρ in synchrony with V_P, then a similar graph is obtained, but with Δt ranging from about 0.17 to 0.47 ms, rather than from 0.12 to 0.53 ms.

AVO calculations

The reflectivity at a boundary of the reservoir is influenced not only by the elastic properties of the reservoir, but also the properties of the bounding media. This information can be obtained from well logs, but in the absence of such, we will assume that the surrounding media are composed of the same rock as the reservoir, but simply contain brine rather than acid gas. Again using data from Table 2 we can calculate the plane-wave Zoeppritz coefficients, with results displayed in Figure 3.

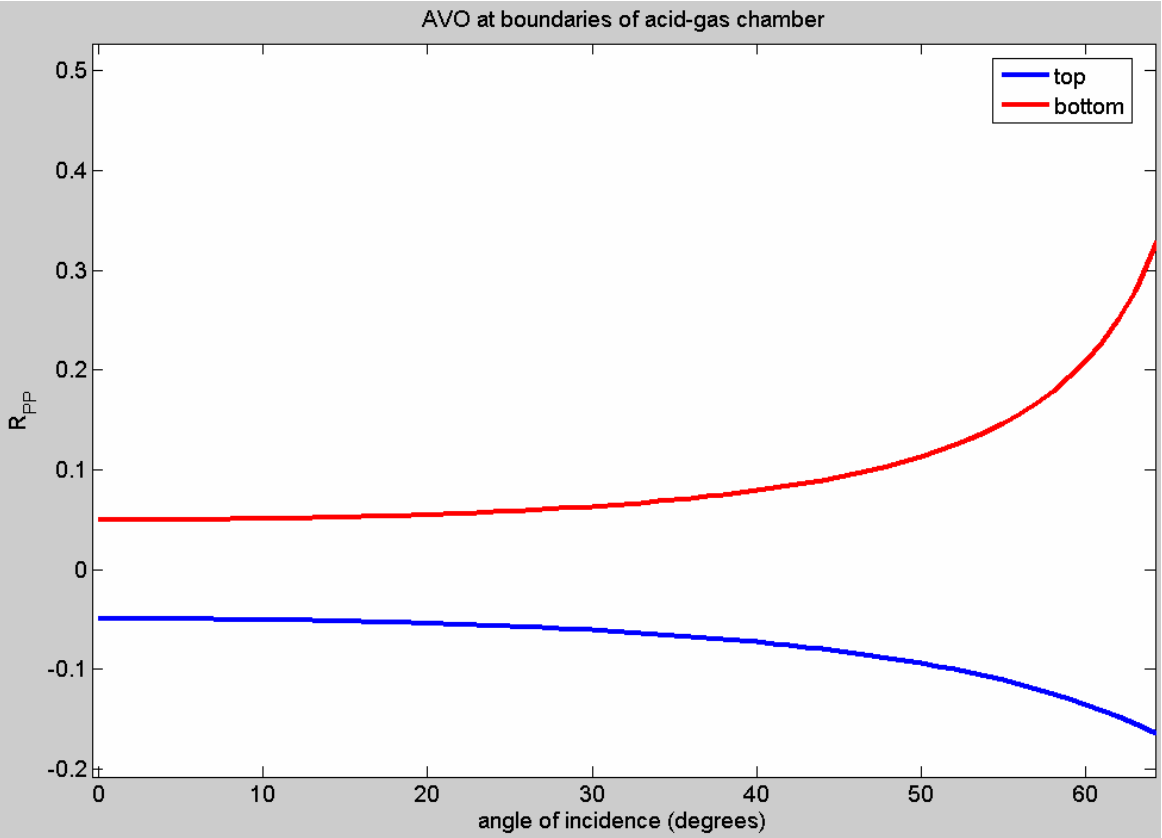

FIG. 3. Reflection coefficient curves defining $R_{PP}(\theta)$ at the top and bottom of an acid gas layer. The rock matrix is assumed to be constant across the interfaces, with brine saturation above and below the reservoir.

The AVO trends shown in Figure 3 do not suggest a very strong response, but more complete modeling with well logs would be required before drawing any final conclusions on the use of AVO for seismic monitoring of this injection.

For completeness, in analogy to Figure 2, we can consider how varying V_P affects $R_{PP}(0)$, and these results are shown in Figure 4. Again, for softer reservoirs, the picture is improved, if only moderately.

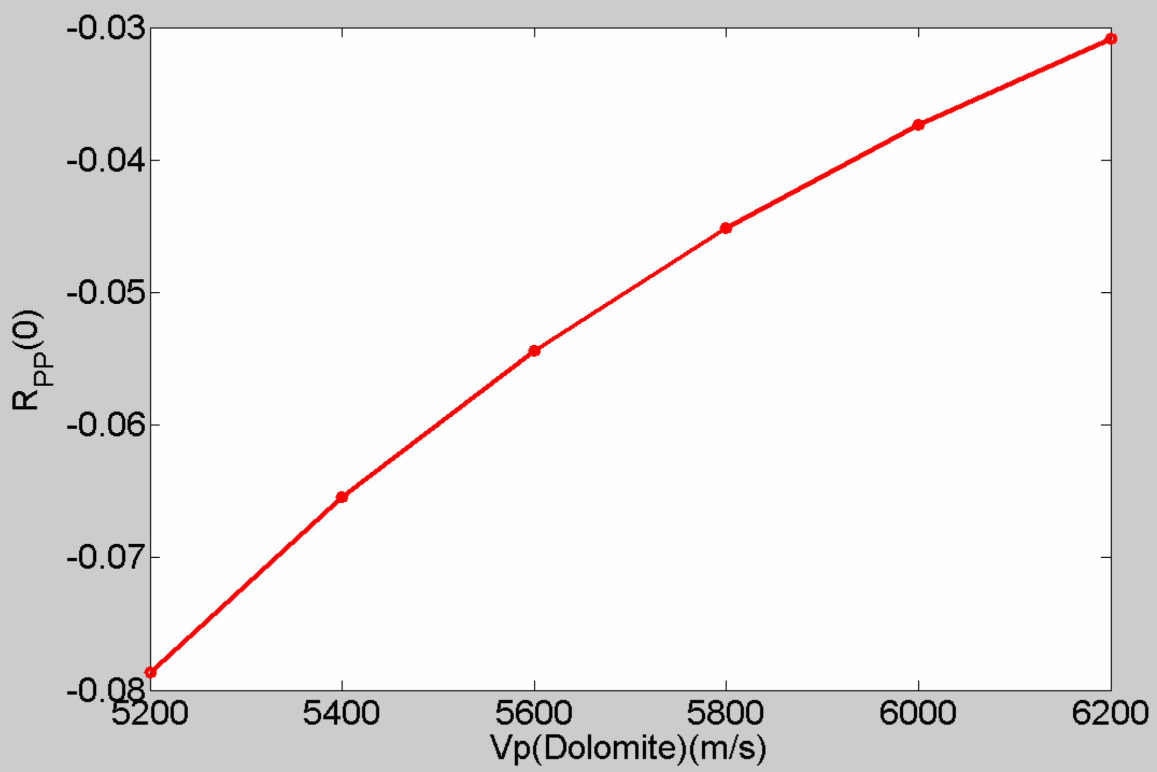

FIG. 4. The effect of reservoir rock V_P on vertical reflectivity [$R_{PP}(0)$] at the top of the injection chamber, given the same assumptions as in Figure 3.

CONCLUSIONS

We have performed calculations relevant to the fluid substitution problem for acid gas injection into a deep saline reservoir. In doing so we have made a number of assumptions:

- The injected acid gas fully displaces the native brine, rather than mixing with it.
- The Gassmann assumptions are satisfied. In particular, the injected acid gas does not react with the dolomite reservoir rock on the timescale of the injection program.
- The properties of the dolomite matrix can be estimated from a range of typical values found in the literature.
- Methane accounts for the fraction of the acid gas which is not CO_2 or H_2S.

Based on these assumptions, we have shown that, for every ten meters thickness in the injection chamber, a vertical seismic signal will likely have a 0.26 ms longer two-way traveltime than through the brine-saturated reservoir. This is based on average properties of dolostone. For dolostone on the softer end of the spectrum, 0.5 ms change is more likely. Changes in reflection amplitudes resulting from fluid substitution do not appear as promising for injection monitoring, but well log based analysis would be necessary to draw firm concluisions.

ACKNOWLEDGEMENTS

The authors gratefully acknowledge the support of CREWES sponsors.

REFERENCES

Batzle, M. and Wang, Z., 1992, Seismic properties of pore fluids: Geophysics, **57**, 1396-1408.

Carroll, J. J., Jou, F.-Y., Mather, A. E. and Otto, F. D., 1992, Phase equilibria in the system water-methyldiethanolamine-propane: AIChE Journal, **38**, 511-520.

Carroll, J. J., 1998, Phase diagrams reveal acid-gas injection subtleties: Oil and Gas Journal, **96**, 92-96.

Carroll, J. J., 2002a, Phase equilibria relevant to acid gas injection, Part 1 – Non-aqueous phase behaviour: Journal of Canadian Petroleum Technology, **41**, No. 6 , 25-31.

Carroll, J. J., 2002b, Phase equilibria relevant to acid gas injection, Part 2 – Aqueous phase behaviour: Journal of Canadian Petroleum Technology, **41**, No. 7, 39-43.

Holloway, S., 2007, Carbon dioxide capture and geological storage: Phil. Trans. R. Soc. A, **365**, 1095-1107.

Mavko, G., Mukerji, T. and Dvorkin, J., 1998, The rock physics handbook: Cambridge University Press.

Peng, D.-Y. and Robinson, D. B., 1976, A new two-constant equation of state: Ind. Eng. Chem., Fundam., **15**, 59-64.

Press, W. H., Flannery, B. P., Teukolsky, S. A., and Vetterling, W. T., 1988, Numerical Recipes: Cambridge University Press.

Reid, R. C., Prausnitz, J. M., and Poling, B. E., 1987, The properties of gases and liquids: Donnelley and Sons.

Sandler, S. I., 1999, Chemical and engineering thermodynamics: Wiley and Sons.

Zhu, X. and McMechan, G. A., 1990, Direct estimation of the bulk modulus of the frame in a fluid-saturated elastic medium by Biot theory: 60th Ann. Internat. Mtg., Soc. Expl. Geophys., Expanded Abstracts.

APPENDIX A – PENG-ROBINSON EQUATION OF STATE

The Peng-Robinson equation of state (Peng and Robinson, 1976; also in numerous chemical engineering textbooks) is given by

$$P = \frac{RT}{v-b} - \frac{a(T)}{v(v+b)+b(v-b)} \tag{A1}$$

where, for a single-component fluid,

$$a(T) = 0.45724\frac{R^2T_c^2}{P_c}\cdot\alpha(T_r,\omega)\ , \tag{A2}$$

$$b = 0.07780\frac{RT_c}{P_c}\ , \tag{A3}$$

$$\alpha^{1/2} = 1+\kappa(1-T_r^{1/2})\ , \tag{A4}$$

$$\kappa = 0.37464 + 1.54226\omega - 0.26992\omega^2 , \tag{A5}$$

$$T_r = T / T_c , \tag{A6}$$

and where T_c (critical temperature), P_c (critical pressure), and ω (acentric factor) are properties tabulated for various compounds (see e.g. Reid et al., 1987).

For a multicomponent fluid, a and b in equations A2 and A3 become subscripted (so that a_i refers to the i^{th} component) and the a and b in equation A1 become defined as

$$a = \sum_i \sum_j x_i x_j (1 - \delta_{ij}) \sqrt{a_i a_j} , \tag{A7}$$

$$b = \sum_i x_i b_i , \tag{A8}$$

where x_i is the mole fraction and δ_{ij} is a binary interaction coefficient, empirically determined for each pair of components (e.g. Sandler, 1999, p. 410).

APPENDIX B – HEAT CAPACITY DEPARTURE

Isobaric heat capacity is defined as the temperature derivative of the enthalpy at constant pressure:

$$C_P = \left(\frac{\partial H}{\partial T} \right)_P . \tag{B1}$$

In this and all other thermodynamic derivatives in this appendix, we will assume implicitly that composition is held fixed as well.

The *heat capacity departure* is the difference between real and ideal (denoted *) heat capacities, at the same temperature, pressure and composition, which we can write as follows:

$$C_P - C_P{*} = (C_P - C_V) - (C_P{*} - C_V{*}) + (C_V - C_V{*}) \tag{B2}$$

where C_V is the isochoric heat capacity. Using standard thermodynamic relations we may replace the three terms in parentheses as follows:

$$C_P - C_P{*} = \frac{TV\alpha^2}{\beta_T} - nR + \left(\frac{\partial (U - U{*})}{\partial T} \right)_V \tag{B3}$$

where T is temperature, V is volume, α is the isobaric thermal expansivity, β_T is the isothermal compressibility, n is the number of moles, R is the ideal gas constant, and U is the internal energy. We will return to equation B3, but first recall that from the First Law of Thermodynamics we have

$$dU = -PdV + TdS \;, \tag{B4}$$

$$\left(\frac{\partial U}{\partial V}\right)_T = -P + T\left(\frac{\partial S}{\partial V}\right)_T , \tag{B5}$$

and, through one of the Maxwell relations,

$$\left(\frac{\partial U}{\partial V}\right)_T = -P + T\left(\frac{\partial P}{\partial T}\right)_V . \tag{B6}$$

For an ideal gas equation B6 reduces to

$$\left(\frac{\partial U^*}{\partial V}\right)_T = -P^* + T\left(\frac{\partial P^*}{\partial T}\right)_V = -\left(\frac{nRT}{V}\right) + T\left(\frac{\partial (nRT/V)}{\partial T}\right)_V = 0 , \tag{B7}$$

so that $U^* = U^*(T)$ is independent of V. Now as a mathematical identity we can write

$$U - U^* = \int_\infty^V \left(\frac{\partial (U-U^*)}{\partial V}\right)_T dV + \left[U(T, V\to\infty) - U^*(T, V\to\infty)\right]. \tag{B8}$$

However $U \to U^*$ as $V \to \infty$ so that the term in square brackets vanishes, and invoking equation B7 then yields

$$U - U^* = \int_\infty^V \left(\frac{\partial U}{\partial V}\right)_T dV = \int_\infty^V \left[-P + T\left(\frac{\partial P}{\partial T}\right)_V\right] dV . \tag{B9}$$

Next apply the isochoric temperature derivative to equation B9 to obtain

$$\left(\frac{\partial (U-U^*)}{\partial T}\right)_V = \int_\infty^V \left[-\left(\frac{\partial P}{\partial T}\right)_V + \left(\frac{\partial P}{\partial T}\right)_V + T\left(\frac{\partial^2 P}{\partial T^2}\right)_V\right] dV . \tag{B10}$$

Now can return to equation B3 which may be expressed as

$$C_P - C_P^* = \frac{TV\alpha^2}{\beta_T} - nR + \int_\infty^V \left[T\left(\frac{\partial^2 P}{\partial T^2}\right)_V\right] dV . \tag{B11}$$

We can perform a change of variables to molar volume, v, in the integration,

$$\int_\infty^V \left[T\left(\frac{\partial^2 P}{\partial T^2}\right)_V\right] dV \;\to\; n\int_\infty^v \left[T\left(\frac{\partial^2 P}{\partial T^2}\right)_v\right] dv , \tag{B12}$$

and then dividing by n yields the molar heat capacity departure,

$$C_{P,m} - C_{P,m}{*} = \frac{Tv\alpha^2}{\beta_T} - R + \int_{\infty}^{v}\left[T\left(\frac{\partial^2 P}{\partial T^2}\right)_v\right]dv\,. \qquad \text{(B13)}$$

This expression is easier to implement with the Peng-Robinson equation of state than the integral over P in Figure 1, as the integral over v can be performed analytically. This expression is given without derivation in Eq. 5-5.3 of Reid (1987).

APPENDIX C –IDEAL MOLAR HEAT CAPACITY

The ideal heat capacity is added to the heat capacity departure to form the full heat capacity. Ideal molar heat capacities for a given compound depend only on temperature and have coefficients for empirical fittings of these functions which have been tabulated for many compounds. A variety of fittings are extant in the literature, each valid over a different temperature range, with varying accuracy. For the small molecules present in acid gas mixtures, it is straightforward to calculate the ideal heat capacities directly from statistical mechanics, and this removes any limits on their use.

First we note that

$$C_{P,m} = C_{V,m} + R \quad \text{(ideal gas),} \qquad \text{(C1)}$$

where R is the ideal gas constant. (All quantities in this appendix refer to the ideal gas.) The isochoric ideal molar heat capacity can be expressed as a sum of translational, rotational, vibrational, and electronic components:

$$C_{V,m} = C_{V,m}^{t} + C_{V,m}^{r} + C_{V,m}^{v} + C_{V,m}^{e}\,. \qquad \text{(C2)}$$

Typical reservoir temperatures are high enough that the equipartition theorem is valid for translational and rotational modes, but low enough that no excited electronic states are populated for typical reservoir species, so these terms contribute simply as follows:

$$C_{V,m}^{t} = \frac{3}{2}R, \qquad \text{(C3)}$$

$$C_{V,m}^{r} = \begin{cases} 0, & \text{monatomic species} \\ R, & \text{linear molecule} \\ (3/2)R, & \text{nonlinear molecule} \end{cases}, \qquad \text{(C4)}$$

$$C_{V,m}^{e} = 0\,. \qquad \text{(C5)}$$

At reservoir temperatures, some higher vibrational levels are populated, but not enough to satisfy equipartition. Therefore we employ the temperature-dependent statistical mechanical expression

$$C_{V,m}^{v} = R\sum_{i}\left(\frac{\eta_i}{\sinh \eta_i}\right)^2 , \tag{C6}$$

$$\eta_i = \frac{1}{2}\frac{\hbar\omega_i}{kT} = \frac{hc}{2kT}\bar{\nu}_i , \tag{C7}$$

where h is Planck's constant, $\hbar = h / (2\pi)$, k is Boltzmann's constant, ω_i is a fundamental vibrational frequency of the molecule, and the wavenumber (commonly used for tabulation of molecular frequencies) is $\bar{\nu}_i = \omega_i/(2\pi c)$. The sum is over all vibrational modes in the molecules, where for a molecule containing M atoms,

$$\text{number of vibrational modes} = \begin{cases} 0, & \text{monatomic species} \\ 3M-5, & \text{linear molecule} \\ 3M-6, & \text{nonlinear molecule} \end{cases} . \tag{C8}$$

In programming equations C1-C8, it is useful to test against an empirical fitting of this function, such as found in Reid et al. (1987) or Sandler (1999).